Quasiparticle anisotropy and pseudogap formation: a weak-coupling renormalization-group analysis

Arno P. Kampf, A.A. Katanin

Angaben zur Veröffentlichung / Publication details:

Kampf, Arno P., and A.A. Katanin. 2006. "Quasiparticle anisotropy and pseudogap formation: a weak-coupling renormalization-group analysis." *Journal of Physics and Chemistry of Solids* 67 (1-3): 146–49. https://doi.org/10.1016/j.jpcs.2005.10.044.

Quasiparticle anisotropy and pseudogap formation: a weak-coupling renormalization-group analysis

A. Kampf [a,*], A. A. Katanin [b,c]

[a] *Institut für Physik, Theoretische Physik III, Universität Augsburg, 86135 Augsburg, Germany*
[b] *Max Planck-Institut für Festkörperforschung, 70569 Stuttgart, Germany*
[c] *Institute of Metal Physics, 62019 Ekaterinburg, Russia*

Abstract

We calculate the self-energy at weak-coupling for the t-t' Hubbard model within the one-loop functional RG approach. At van Hove (vH) band fillings the quasiparticle (qp) concept is found invalid at $\mathbf{k}_F = (\pi, 0)$. At low temperature the qp weight along the Fermi surface continuously vanishes from a finite value at the zone diagonal towards the $(\pi, 0)$ point. Away from vH band fillings the qp peak is formed inside a pseudogap of size Δ, and within a finite frequency window $|\omega| \ll \Delta$ around the Fermi energy the electronic self-energy has the conventional Fermi-liquid form. With increasing separation between Fermi level and vHs the spectral anomalies gradually disappear.

Key words: Pseudogap, quasiparticles, renormalization-group
PACS: 71.10.Fd, 71.27.+a, 74.25.Dw

Non-Fermi-liquid (nFL) normal state properties, pseudogap formation, and the absence of well-defined qps near the $(\pi, 0)$ point of the Brillouin zone (BZ) belong to the most intriguing phenomena of high-T_c cuprates. The existing theories have related the origin of the pseudogap to precursors of antiferromagnetism (AFM) [1], preformed pairs [2], or to the onset of orbital currents [3]. The absence of qps near the $(\pi, 0)$ point was connected to a partial disappearance of the Fermi surface (FS) and the existence of hole pockets near the BZ diagonal [4]. Without pretending for a complete description of cuprate materials, model studies of pseudogap formation and its connection to the violation of the FL qp concept pose a challenging problem for correlated electron theory.

In the conventional FL, the self-energy at the Fermi wavevector $\mathbf{k}_F$ behaves at small frequencies as $\mathrm{Re}\Sigma(\mathbf{k}_F, \omega) \simeq \mathrm{const} + (1 - 1/Z)\omega, \mathrm{Im}\Sigma(\mathbf{k}_F, \omega) \simeq -(1/\tau + B\omega^2)$ where $Z < 1$ and $\tau \sim 1/T^2$ denote the qp weight and lifetime. The appearance of a pseudogap in the spectral function necessarily requires additional structure in the self-energy to account for the suppression of spectral weight near the Fermi level.

The pseudogap formation due to AFM correlations was investigated in the one-band 2D Hubbard model using the fluctuation exchange (FLEX) [5,6], two-particle self-consistent (TPSC) approx-

* Corresponding author
Email address: kampfa@physik.uni-augsburg.de (A. Kampf).

imations [7] and the dynamical cluster approximation (DCA) [8]. The FLEX results showed the crossover to a nFL form of the self-energy at half filling $n = 1$ upon cooling [5], but for $n < 1$ FLEX detects only a variation of the qp weight around the FS [6]. QMC studies provided reliable insight into the doping evolution of the spectral function in the strong to intermediate coupling regime [9], but were not able to trace the pseudogap formation in the weak-coupling regime.

Recently, renormalization-group (RG) approaches on a patched FS [10–12] were developed as a new tool to investigate the instabilities of interacting electron systems. RG studies focused mostly on two-particle properties, e.g. selected order parameter susceptibilities. Although the electronic on-shell lifetime and the qp spectral weight [13] were also recently considered within the many-patch RG analysis, these quantities alone are only indicative but not sufficient to tell, whether the FL concept remains valid.

In the present paper we use the RG scheme for the t-t' weak-coupling Hubbard model to calculate the self-energy by analytical continuation from the imaginary frequency axis. $\Sigma(\mathbf{k}_F, i\omega_n)$ is obtained with the vertices obtained in the one-loop RG approach. We show that at vH band fillings the qp weight along the FS continuously vanishes from a finite value at the BZ diagonal towards the $(\pi, 0)$ point where the qp concept is invalid. The qp weight suppression is accompanied by the growth of two additional incoherent peaks in the spectral function, from which the anisotropic pseudogap originates. On moving away from vH band fillings, the qp peak is formed inside the pseudogap and its spectral weight grows, while the self-energy approaches its conventional FL form.

Specifically, we consider the Hubbard model for N_e electrons on a square lattice

$$H = -\sum_{ij\sigma} t_{ij} c^\dagger_{i\sigma} c_{j\sigma} + U \sum_i n_{i\uparrow} n_{i\downarrow} - \mu N_e \qquad (1)$$

where $t_{ij} = t$ for nearest neighbor (nn) sites i and j and $t_{ij} = -t'$ for next-nn sites ($t, t' > 0$); for convenience we have shifted the chemical potential $\mu = \tilde{\mu} - 4t'$. We apply the RG approach for one particle-irreducible (1PI) functions [11] with a

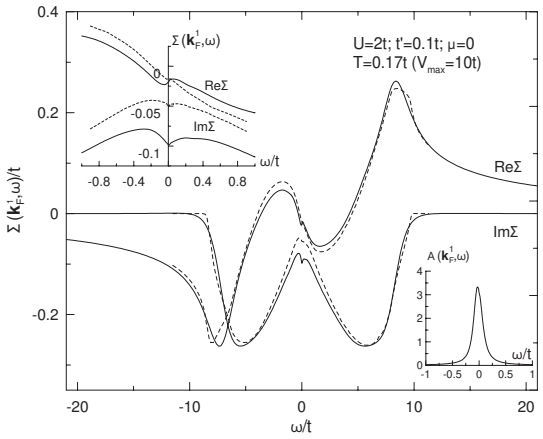

Fig. 1. Self-energy in SOPT (dashed) and the one-loop RG approach (solid line) at $U = 2t$, $t'/t = 0.1$, and vH band filling n=0.92 at $T = 0.17t$ ($V_{max} = 10t$). $\mathbf{k}^1_F$ is chosen in the first patch, closest to the vHs. The insets show the self-energy and the spectral function at small frequencies.

sharp momentum cutoff [13], which considers the effective action obtained by integrating out modes with energy $|\varepsilon_\mathbf{k}| \geq \Lambda$, where $\varepsilon_\mathbf{k}$ is the electronic dispersion; Λ ($0 < \Lambda < \Lambda_0 = \max|\varepsilon_\mathbf{k}|$) is the cutoff parameter. This procedure is used in the weak-coupling regime for $t' \lesssim 0.3t$ [12]. The flow of the self-energy $\Sigma_\Lambda(\mathbf{k}, i\omega)$ in the 1PI RG scheme is given by $\mathrm{d}\Sigma_\Lambda/\mathrm{d}\Lambda = V_\Lambda \circ S_\Lambda$, where $\circ$ is a short notation for the summation over momentum-, frequency- and spin-variables, see e.g. Ref. [13]. The renormalization of the interaction vertex V_Λ at one-loop order is given by

$$\frac{dV_\Lambda}{d\Lambda} = V_\Lambda \circ (G_\Lambda \circ S_\Lambda + S_\Lambda \circ G_\Lambda) \circ V_\Lambda. \qquad (2)$$

The propagators G_Λ and S_Λ are defined by

$$\left\{ \begin{array}{c} G_\Lambda \\ S_\Lambda \end{array} \right\} (\mathbf{k}, i\omega_n) = \left\{ \begin{array}{c} \theta(|\varepsilon_\mathbf{k}| - \Lambda) \\ \delta(|\varepsilon_\mathbf{k}| - \Lambda) \end{array} \right\} \frac{1}{i\omega_n - \varepsilon_\mathbf{k}}. \qquad (3)$$

We neglect the influence of the self-energy on the RG flow and therefore the self-energy is not included in the Green functions (3). $\mathrm{d}\Sigma/\mathrm{d}\Lambda = V_\Lambda \circ S_\Lambda$ and Eq. (2) have to be solved with the initial conditions $V_{\Lambda_0} = U$ and $\Sigma_{\Lambda_0} = 0$. Since the frequency dependence of the vertices is neglected, it is convenient to reinsert the vertex from Eq. (2) into $\mathrm{d}\Sigma/\mathrm{d}\Lambda = V_\Lambda \circ S_\Lambda$ to obtain [13]

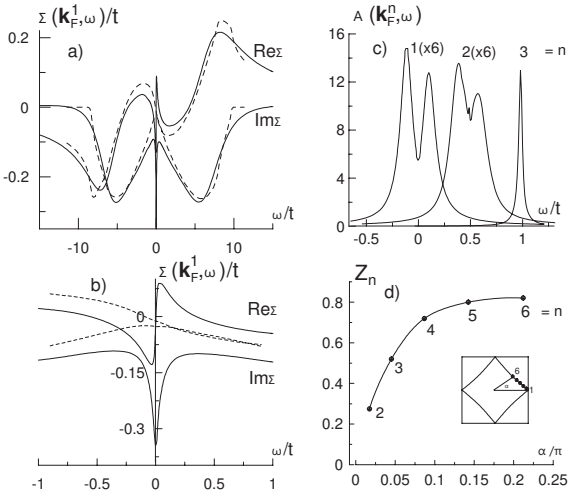

Fig. 2. Same as Fig. 1 for $T = 0.082t$ ($V_{max} = 100t$). In addition, c) and d) show the spectral functions and the qp weights for $\mathbf{k}_F^n$ in different patches around the FS. The spectral functions are shifted by $(n-1)0.5t$ for a better view; for $n = 1, 2$ they are multiplied by 6.

$$\frac{d\Sigma_\Lambda}{d\Lambda} = S_\Lambda \circ \int_\Lambda^{\Lambda_0} \mathrm{d}\Lambda' [V_{\Lambda'} \circ (\quad G_{\Lambda'} \circ S_{\Lambda'} + S_{\Lambda'} \circ G_{\Lambda'}) \circ V_{\Lambda'}]. \quad (4)$$

To solve Eqs. (2) and (4) numerically we divide the momentum space into 48 patches with the same patching scheme as in Refs.[11,12]. The self-energy on the real axis is obtained by analytical continuation using Padé approximants. To resolve fine structures close to the Fermi level, we use a dense set of frequencies on the imaginary axis at small $|\omega| \lesssim t$ and a set of $i\omega_n$ for $|\omega| \gg t$. The quality of the Padé approximants was checked by both the analysis of the analyticity in the upper half-plane and by requiring the fulfillment of the sum rule for the resulting Green function.

First we consider the results at the vH band filling ($\mu = 0$) for $t' = 0.1t$ and $U = 2t$. The self-energy at temperature $T = 0.17t$ calculated within RG together with the self-energy in second-order perturbation theory (SOPT, obtained by the replacement $V \to U$ in Eq. (4)) is shown in Fig. 1. Remarkably, in the first patch, which is closest to the vHs at $(\pi, 0)$, SOPT and RG results show both a minimum of $\mathrm{Im}\Sigma(\mathbf{k}_F, \omega)$ at the Fermi level instead of a maximum as expected for a FL. Simultaneously, $\mathrm{Re}\Sigma(\mathbf{k}_F, \omega)$ has a positive slope near $\omega = 0$. The dip in $\mathrm{Im}\Sigma$ calculated within RG is much more pronounced than in SOPT. The peculiarities of the SOPT self-energy arise solely from the thermal excitation of electrons near the vHs and exist at all $T > 0$ decreasing in size with decreasing T so that the conventional structure of Σ is recovered in the $T \to 0$ limit. Instead, the more pronounced anomalies in the RG self-energy increase in size with decreasing T and reflect the tendency towards pseudogap formation. Importantly, the single peak in $A(\mathbf{k}_F, \omega) = -\mathrm{Im}G(\mathbf{k}_F, \omega)/\pi$ in Fig. 1 is not a qp feature because the low energy structure of Σ invalidates the qp concept. Outside the first patch, the real part of the self-energy has a narrow region with negative slope near $\omega = 0$, while for larger $|\omega|$ the behavior is qualitatively similar in all patches. With increasing T to $\sim 0.5t$ the interaction vertices are only weakly renormalized and the self-energy almost coincides with the SOPT result.

In Fig. 2 we decrease T to $0.082t$ which is closer to the crossover scale T^*, where the one-loop interaction vertices V tend to diverge [11]. Although the low-T regime where the effective vertices are so large ($V_{\max} = 100t$) is outside the validity region of the one-loop approach, it proves most useful to clearly identify the structure of the spectral function. In the first patch a two-peak structure in $A(\mathbf{k}_F, \omega)$ arises with a local minimum at the Fermi energy, while in the other patches at nonzero t' a qp peak exists at the Fermi energy. This peak quickly merges with the two incoherent peaks of the pseudogap on approaching the BZ diagonal. The qp weight around the FS (see Fig. 2d) gradually vanishes with approaching the $(\pi, 0)$ point. For $t' = 0$ and the corresponding vH band filling $n = 1$, the qp peak is absent in all patches. All spectral functions along the FS show in this case a two-peak pseudogap structure at low T similar to the TPSC [7] and DCA [8] results.

In Figs. 3a,c we show the self-energy for $U = 2t$, $t' = 0.1t$ and $\mu = 0.03t$ ($n = 0.94$) so that the Fermi level is slightly above the vHs energy. At $T = 0.18t$ only weak anomalies in $\Sigma(\mathbf{k}_F^1, \omega)$ are present near the Fermi level. Upon lowering the temperature towards T^* a clear maximum of $\mathrm{Im}\Sigma$ develops. The real part of the self-energy has a negative slope in a narrow energy window $|\omega| \lesssim \mu$.

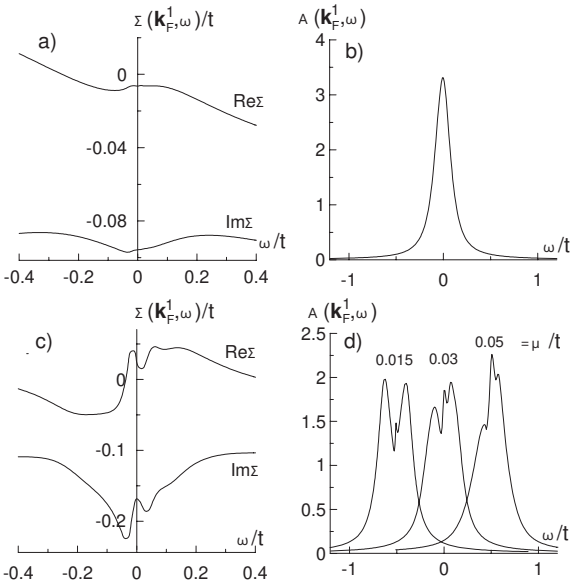

Fig. 3. Self-energy (a,c) and quasiparticle spectral weight (b,d) for a patch closest to the vHs at $U = 2t$, $t'/t = 0.1$, $\mu = 0.03t$, $T = 0.18t$ ($V_{max} = 10t$; a,b) and $T = 0.09t$ ($V_{max} = 100t$; c,d). (d) shows the evolution of the spectral weight for different μ. The curves are shifted by $0.5t$ for a better view.

In the spectral function we observe the split-off of two incoherent peaks near the qp peak at the Fermi level (Fig. 3d). For larger μ, the qp peak regains its weight from the incoherent pseudogap peaks and when μ is of the order of the maximum size of the pseudogap Δ, a single peak in the spectral function remains. The picture described above for $\mu > 0$ is observed also for $\mu < 0$, but in this case for finite t' the value of T^* fastly decays with $|\mu|$ and the single-peak structure of the spectral function sets in much earlier than for $\mu > 0$.

In conclusion, we have investigated the self-energy on the real frequency axis in the $2D$ t-t' Hubbard model at and near vH fillings within a one-loop RG analysis. For vH fillings the self-energy has a non-FL form at the FS point $(\pi, 0)$. Qps exist everywhere else on the FS but with anisotropic spectral weight. The RG flow indicates that at low T the continuous decrease of the qp weight along the FS is accompanied by the simultaneous growth of two additional incoherent peaks in the spectral function. Away from vH fillings the qp peak is restored, its weight continuously increases with increasing $|\mu|$, and for $|\mu| \gg \Delta$ the conventional qp concept is recovered.

These RG results near vH fillings provide a novel scenario for the anisotropic spectral properties and low-T pseudogap formation in the 2D t-t' Hubbard model. The observed features are distinctly different from the previously found low-T crossover to a non-FL form of Σ at half filling as well as from the proposed hole pocket picture and the partial destruction of the FS in strong coupling Hubbard or $t - J$ models. Despite the fact that the weak-coupling RG analysis is applicable only outside the parameter regime considered relevant for cuprate materials, the results offer a valid alternative for the interpretation of experimental data from photoemission spectroscopy.

This work was supported by the Deutsche Forschungsgemeinschaft through SFB 484.

References

[1] J. Schmalian et al., Phys. Rev. Lett. **80**, 3839 (1998); Phys. Rev. B **60**, 667 (1999); Ar. Abanov et al., Adv. Phys. **52**, 119 (2003).

[2] V. Emery and S. Kivelson, Phys. Rev. Lett. **74**, 3253 (1995); Nature **374**, 434 (1995).

[3] C. M. Varma, Phys. Rev. B **55**, 14554 (1997).

[4] X.-G. Wen and P. A. Lee, Phys. Rev. Lett. **76**, 503 (1996); A. V. Chubukov and D. K. Morr, Phys. Rep. **288**, 355 (1997).

[5] J. Deisz et al., Phys. Rev. Lett. **76**, 1312 (1996).

[6] J. Altmann et al., Eur. Phys. J. B **18**, 429 (2000).

[7] J. Vilk and A.-M. S. Tremblay, J. Phys. I **7**, 1309 (1997); B. Kyung, Phys. Rev. B **58**, 16032 (1998).

[8] C. Huscroft et al., Phys. Rev. Lett. **86**, 139 (2001).

[9] S. R. White, Phys. Rev. B **44**, 4670 (1991); N. Bulut et al., Phys. Rev. Lett. **72**, 705 (1994).

[10] D. Zanchi and H. J. Schulz, Phys. Rev. B **54**, 9509 (1996); ibid. **61**, 13609 (2000); C. J. Halboth and W. Metzner, ibid. **61**, 7364 (2000); Phys. Rev. Lett. **85**, 5162 (2000).

[11] M. Salmhofer and C. Honerkamp, Progr. Theor. Phys. **105**, 1 (2001).

[12] C. Honerkamp and M. Salmhofer, Phys. Rev. Lett. **87**, 187004 (2001); Phys. Rev. B **64**, 184516 (2001).

[13] C. Honerkamp, Eur. Phys. J. B **21**, 81 (2001).